

Phase Equilibria in the Ag–In–Pd System at 700°C

Adéla Zemanová¹, Olga Semenova², Aleš Kroupa³, Jan Vřešťál^{1,*}, Karthik Chandrasekaran², Klaus W. Richter², and Herbert Ipser²

¹ Institute of Theoretical and Physical Chemistry, Faculty of Science, Masaryk University, 611 37 Brno, Czech Republic

² Institut für Anorganische Chemie, Universität Wien, A-1090 Wien, Austria

³ Institute of Physics of Materials, Academy of Sciences of Czech Republic, 616 62 Brno, Czech Republic

Received September 12, 2004; accepted November 26, 2004

Published online November 14, 2005 © Springer-Verlag 2005

Summary. Phase equilibria in the Ag–In–Pd system were determined at 700°C based on experimental results for 21 alloys. A ternary compound T₁ (with the approximate composition AgInPd₂) was identified by XRD analysis. These data were compared with the results of a CALPHAD-type prediction, based on binary thermodynamic data only and a symmetrical *Redlich–Kister–Muggianu* model. The experimental results will serve as a basis for refined thermodynamic modeling of the different phases in this ternary system.

Keywords. Phase diagrams; Thermodynamics; X-ray structure determination; Ag–In–Pd system.

Introduction

The aim of this contribution is to study the Ag–In–Pd system as one of the limiting ternaries of the Ag–In–Pd–Sn quaternary system, which is important for the understanding of contacts between lead-free Sn–Ag–In solders and Pd containing substrates. In a first step, the Ag–In–Pd phase diagram is predicted by means of the so-called CALPHAD method [1] based on thermodynamic data for the binary systems, starting with an isothermal section at 700°C. Unary and binary thermodynamic data for all three binary systems are taken from the COST531 database which is currently being compiled [2]. In a second step, the calculated isotherm is compared with experimental data for some critical concentrations. A combination of powder X-ray diffractometry (XRD), metallography, electron-probe microanalysis (EPMA), and scanning electron microscopy (SEM), equipped with an EDAX analyzer, is used for identification of phases and phase equilibria.

* Corresponding author. E-mail: vrestal@chemi.muni.cz

Thermodynamic Modeling

Pure Elements

The pure solid elements at 298.15 K and 1 bar in their stable forms were chosen as the reference state of the systems (SER). The SGTE 4.4 (Scientific Group Thermo-data Europe) database of phase stabilities, for stable and metastable states of pure elements, compiled by *Dinsdale* [3] was used.

The Binary Systems

The thermodynamic description of the binary alloys was taken from the literature. Optimized thermodynamic functions for the Ag–In system were published in Ref. [4], for the Ag–Pd system in Ref. [5], and thermodynamic data for the In–Pd system were taken from Ref. [6]. All these data are included in Ref. [2].

Liquid and Solid Solution Phases

The *Gibbs* energies of liquid, hcp and fcc solid phases are described by the sub-regular solution model with a *Redlich–Kister* polynomial [7] as follows by Eqs. (1)–(3) where ${}^mL_{A,B}^\varphi$ is a temperature-dependent interaction parameter optimized on the basis of the available thermodynamic and phase diagram data, and A, B are elements of the system.

$$G_m^\varphi = {}^\circ G_A^\varphi x_A^\varphi + {}^\circ G_B^\varphi x_B^\varphi + RT(x_A^\varphi \ln x_A^\varphi + x_B^\varphi \ln x_B^\varphi) + G^E(T, x_B) \quad (1)$$

$$G^E(T, x_B) = x_A^\varphi x_B^\varphi L_{A,B}^\varphi \quad (2)$$

$$L_{A,B}^\varphi = \sum_{m=0}^n {}^m L_{A,B}^\varphi (x_A - x_B)^m \quad (3)$$

All other symbols are used in accord with the definitions used traditionally in the CALPHAD method (see *e.g.* Ref. [8]).

Since the Ag–Pd phase diagram is characterized by complete miscibility in the liquid and the solid state it is treated accordingly.

Stoichiometric Compounds in the Ag–In System

The solubility of the compound phases in this system is very small and not clearly determined according to the literature. The phases Ag_2In and AgIn_2 are treated as stoichiometric compounds; then, the *Gibbs* energy of the compound, Ag_mIn_n , is described as given by Eq. (4) where $\Delta G_{\text{Ag}_m\text{In}_n}^f$ represents the *Gibbs* energy of formation per mol of atoms of the compound Ag_mIn_n and is expressed by Eq. (5).

$$G_m^{\text{Ag}_m\text{In}_n} = \frac{m}{m+n} {}^\circ G_{\text{Ag}}^{\text{fcc}} + \frac{n}{m+n} {}^\circ G_{\text{In}}^{\text{fcc}} + \Delta G_{\text{Ag}_m\text{In}_n}^f \quad (4)$$

$$\Delta G_{\text{Ag}_m\text{In}_n}^f = A + BT \quad (5)$$

The Compounds in the In–Pd System

The B2 Compound

InPd is a B2 compound with triple-defects, *i.e.*, constitutional vacancies on the Pd sublattice and antisite Pd atoms on the In sublattice, and it is described by an (In,Pd)_{0.5}(Pd,Va)_{0.5} two-sublattice model [6]. The *Gibbs* energy per mol of formula unit is written as shown by Eq. (6) where y_i^I and y_i^{II} are the site fractions of species i on the first and second sublattice, respectively, and L are the interaction parameters and can be both composition and temperature dependent.

$$G_m = y_{\text{In}}^I y_{\text{Pd}}^{II} \circ G_{\text{In:Pd}} + y_{\text{In}}^I y_{\text{Va}}^{II} \circ G_{\text{In:Va}} + y_{\text{Pd}}^I y_{\text{Pd}}^{II} \circ G_{\text{Pd:Pd}} + y_{\text{Pd}}^I y_{\text{Va}}^{II} \circ G_{\text{Pd:Va}} \\ + 0.5RT(y_{\text{In}}^I \ln y_{\text{In}}^I + y_{\text{Pd}}^I \ln y_{\text{Pd}}^I) + 0.5RT(y_{\text{Pd}}^{II} \ln y_{\text{Pd}}^{II} + y_{\text{Va}}^{II} \ln y_{\text{Va}}^{II}) \\ + y_{\text{In}}^I y_{\text{Pd}}^I (y_{\text{Pd}}^{II} L_{\text{In,Pd:Pd}} + y_{\text{Va}}^{II} L_{\text{In,Pd:Va}}) + y_{\text{Pd}}^I y_{\text{Va}}^{II} (y_{\text{In}}^I L_{\text{In:Va}} + y_{\text{Pd}}^I L_{\text{Pd:Va}}) \quad (6)$$

The composition dependence is described by the *Redlich–Kister* [7] model; and $\circ G_{i;j}$ is the *Gibbs* energy of the compound, with the first sublattice entirely occupied by species i , and the second entirely by j , be it real or hypothetical. Based on the mathematical equivalence between the *Wagner–Schottky* model and the sublattice model [9], the following constraint is imposed in order to decrease the number of model parameters to be optimized (Eq. (7)).

$$\circ G_{\text{In:Pd}} + \circ G_{\text{Pd:Va}} = \circ G_{\text{In:Va}} + \circ G_{\text{Pd:Pd}} \quad (7)$$

The value of $\circ G_{\text{In:Va}}$ is assumed to be $0.5 \cdot \circ G_{\text{In}}^{\text{bcc}} + 5000 - 0.5 \cdot T$ following the treatment of the NiAl (B2) phase by *Ansara et al.* [10].

Other Compounds in the In–Pd System

The compounds In₇Pd₃, In₃Pd₂, In₃Pd₅, α -InPd₂, and α -InPd₃, with negligible homogeneity ranges, were modeled as stoichiometric compounds in the same way as in the case of Ag–In compounds.

Prediction of Phase Equilibria in the Ternary Ag–In–Pd System at 700°C

Virtually no experimental information on phase equilibria and thermodynamics of the Ag–In–Pd ternary system was available in the literature except for a very limited isopleth by *Suh et al.* [11]. Therefore, the ternary phase diagram was calculated, based only on the data for the pure elements from Ref. [3] and for the binary thermodynamic properties from Refs. [4–6] using the *Redlich–Kister–Muggianu* model for the thermodynamic functions. The isothermal section at 700°C predicted in this way is shown in Fig. 1.

Experimental Ag–In–Pd Isothermal Section at 700°C

The phase equilibria in the ternary Ag–In–Pd system were studied by a combination of powder X-ray diffractometry (XRD), metallography, electron-probe micro-

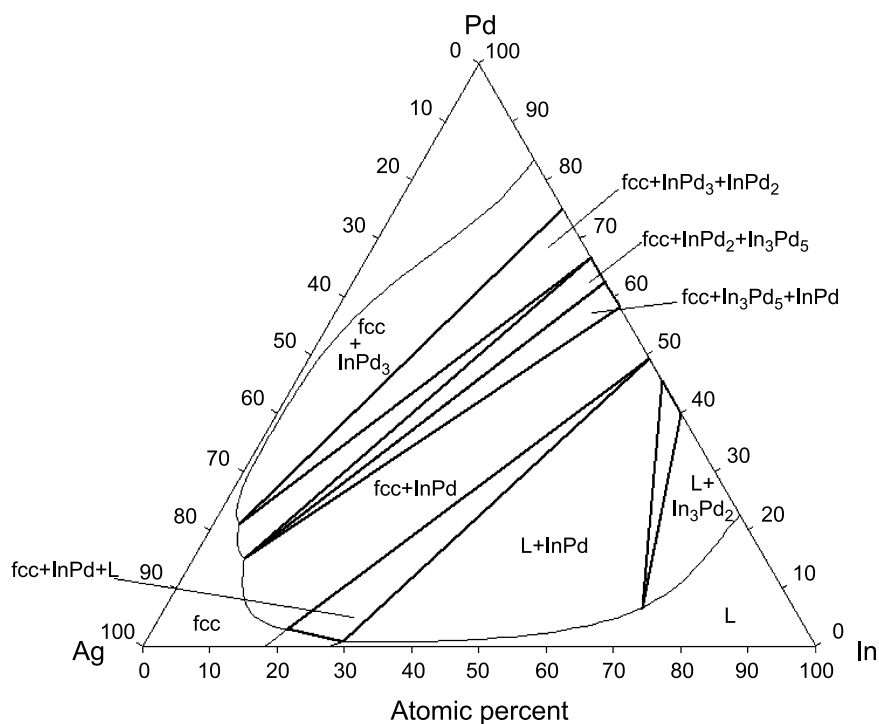


Fig. 1. Phase equilibria at 700°C: CALPHAD-type calculation based on binary data only

analysis (EPMA), and scanning electron microscopy (SEM) equipped with an EDAX analyzer.

A first set of ternary alloys was prepared in Vienna and their overall compositions are given in Table 1 (first series). Most of them were investigated by EPMA, and the various phases were identified by XRD analysis based on the well known patterns of the binary compounds. In addition, the presence of a ternary compound T_1 (with an approximate composition AgInPd_2 and a certain homogeneity range) was reliably confirmed. A second set of samples, with compositions chosen in the predicted three-phase regions, was prepared in Brno in order to verify the phase equilibria calculated for 700°C based on the binary information only. Their overall compositions are also included in Table 1 (second series). The microstructure of these samples, annealed at 700°C, was studied by means of SEM (equipped with an EDAX analyzer), some were also studied by XRD.

So, all experimental results are collected in Table 1, and the corresponding isothermal section at 700°C, based on these experimental results, is shown in Fig. 2.

Comparison of the Experimental Phase Diagram with the Prediction Based on Thermodynamic Data of Binary Systems

As mentioned above, the phase diagram calculations represented in Fig. 1 were based on binary data only. Thus it is not surprising that the experimental phase diagram is in disagreement with the theoretical calculations, because the prediction

Table 1. Composition of the phases in the investigated samples (by EPMA or SEM) together with results of XRD

Sample	Overall composition		Phases identified	Phase compositions	
	at.% Ag	at.% In		at.% Ag	at.% In
First series of samples (compositions by EPMA/Vienna)					
1C	46.9	42.9	L	a	a
			InPd	3.9	53.6
2C	41.1	38.2	L	a	a
			InPd	12.3	45.7
3C	35.2	33.6	fcc	84.8	13.2
			InPd	10.2	44.0
4C	31.3	28.9	fcc	94.4	1.7
			InPd	15.6	34.6
5C	24.7	24.0	fcc, InPd, T ₁	a	a
1D	22.4	62.8	L, In ₃ Pd ₂	a	a
2D	19.9	56.0	In ₃ Pd ₂	a	a
			L	57.8	35.8
3D	17.6	49.1	L, InPd	a	a
4D	15.3	41.7	fcc	80.4	16.8
			InPd	14.1	43.5
5D	12.6	35.0	InPd	a	a
1F	22.8	24.6	InPd	18.6	29.9
			T ₁	19.5	25.6
			fcc	88.6	1.4
3F	29.9	20.2	InPd ₃	3.8	22.2
			fcc	34.3	7.6
4F	29.6	20.3	T ₁	17.1	24.3
			fcc	83.0	1.4
6F	19.7	30.2	InPd	a	a
7F	22.5	22.5	T ₁	a	a
8F	27.5	27.3	InPd	17.9	31.3
			fcc	90.0	1.6
Second series of samples (compositions by SEM/Brno)					
2D'	20.0	56.7	L	33.7	65.7
			InPd	3.5	52.3
			In ₃ Pd ₂	1.6	57.6
5C'	23.4	23.8	(T ₁) ^b	19.3	25.2
			InPd	16.8	30.2
			fcc	82.2	3.5
5D'	10.7	33.8	InPd	a	a
8B	2.9	39.9	InPd	a	a
9B	42.7	30.5	InPd	11.1	43.6
			fcc	82.0	15.0

^a Composition not determined by EPMA or SEM, solid phases identified by XRD; ^b the composition corresponds to the ternary phase T₁, confirmation by X-ray diffraction has not been obtained yet

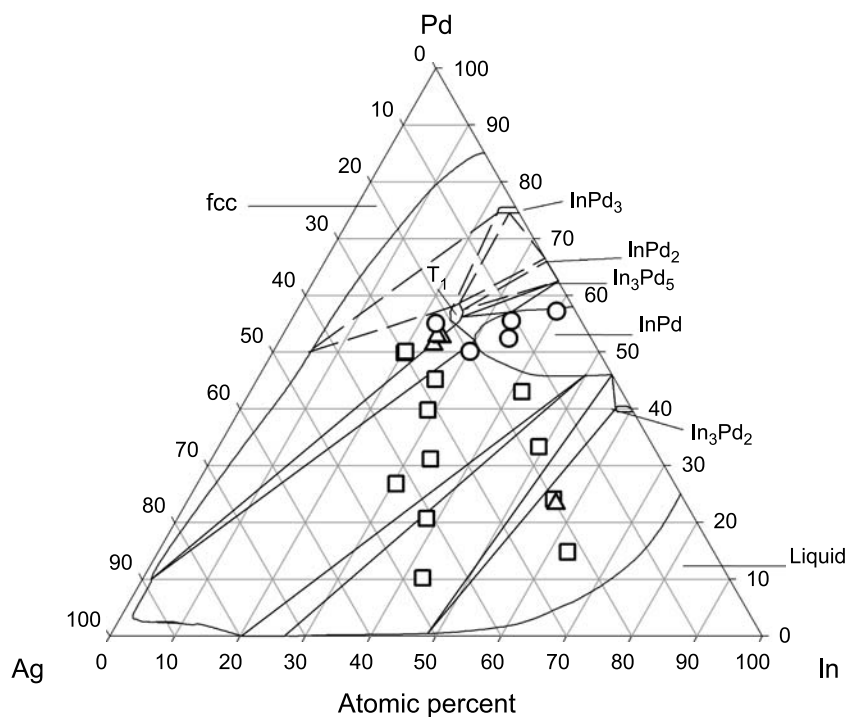


Fig. 2. Phase equilibria at 700°C based on the experimental results in Table 1: O, single phase; □, two-phase; Δ, three-phase

does not include the solubility of any third element in intermetallic phases of the corresponding binary system. The experimental results show that the solubility of Ag in the InPd, InPd₃, and In₃Pd₂ is high. The solubility of Ag in InPd phase is as much as 20%, it is about 2% in In₃Pd₂, and the intermetallic phase InPd₃ contains about 4% Ag. The phase InPd₂ was not found in the experiments and therefore no information about the solubility exists.

The existence of a ternary phase T₁ (see Fig. 2) was confirmed by XRD. Of course, this phase could not be predicted by the described phase diagram calculations. As a consequence, the CALPHAD type calculations need to be improved in order to consider all experimental phase equilibrium data.

Experimental

All samples were prepared from pure Ag (99.98%), In (99.999%), and Pd (99.95%) by induction melting under an Ar atmosphere. They were annealed in evacuated quartz capsules at 700°C, the first series for six weeks, the second series first for 24 hours and then for one additional week. The heat treatment was always finished by water quenching. The samples for EPMA and SEM underwent the standard metallographic surface preparation procedure.

EPMA on polished samples of the first set was carried out on a Cameca SX 100 electron probe (Cameca, Courbevoie, France) applying wavelength dispersive spectroscopy (WDS). The beam current was 20 nA at a voltage of 15 kV. For quantitative analysis Ag L_β, In L_β and Pd L_α characteristic X-ray lines were used. Pure Ag and Pd as well as the stoichiometric compound InSb served as standard materials for quantitative analysis. The microstructure of the samples of the second series was studied

by means of a JEOL JSM-6460 SEM equipped with an EDAX analyzer, using an accelerating potential of 20 kV.

XRD powder diffraction patterns were obtained in a *Guinier–Huber* film chamber using Cu $K_{\alpha 1}$ radiation and employing an internal standard of high purity Si for precise lattice parameters determination. The heat-treated samples were powdered and stress-annealed. The exposure time was 20 h. The TREOR software was used for the evaluation of diffraction lines [12]. A few samples of the second series were investigated by XRD using the diffractometer Philips/PANalytical X’Pert PRO.

Acknowledgements

This research is a contribution to COST Action 531. The authors are grateful to the Ministry of Education of the Czech Republic (Projects No. COST OC 531.001 and OC 531.002) and to the Austrian Science Foundation (FWF, Project No. 15630) for financial support.

References

- [1] See for example: a) Chang YA, Chen Sh, Zhang F, Yan X, Xie F, Schmid-Fetzer R, Oates WA (2004) *Prog Mater Sci* **49**: 313; b) entire issue 2 (1997) *CALPHAD* **21**: 139–287
- [2] Version 1.1 of the COST531 Database for Lead Free Solders
- [3] Version 4.4 of the SGTE Unary Database
- [4] Moser Z, Gasior W, Pstrus J, Zakulski W, Ohnuma I, Liu XJ, Inohana Y, Ishida K (2001) *J Electron Mater* **30**: 1120
- [5] Ghosh G, Kantner C, Olson GB (1999) *J Phase Equilibria* **20**: 295
- [6] Jiang Ch, Liu Z-K (2002) *Met Mater Trans* **33A**: 3597
- [7] Redlich O, Kister AT (1948) *Ind Eng Chem* **24**: 345
- [8] Saunders N, Miodownik AP (1998) *CALPHAD (calculation of phase diagrams): A Comprehensive Guide*. Elsevier, vol 1. London, p 479
- [9] Dupin N, Ansara I (1993) *J Phase Equilibria* **14**: 451
- [10] Ansara I, Dupin N, Lukas HL, Sundman B (1997) *J Alloys Compounds* **247**: 20
- [11] Suh YC, Lee ZH, Ohta M (2000) *J Mater Sci: Mater Med* **11**: 301
- [12] Werner P-E, Eriksson L, Westdahl M (1985) *J Appl Cryst* **18**: 367